Journal of Geoscience and Environment Protection, 2022, 10, 43-61
https://www.scirp.org/journal/gep
ISSN Online: 2327-4344
ISSN Print: 2327-4336

Land Cover Dynamics and Assessment of the Impacts of Agricultural Pressures on Wetlands Based on Earth Observation Data: Case of the Azagny Ramsar Site in Southern Côte d'Ivoire

Kadio Saint Rodrigue Aka[1*], Hyppolite N'da Dibi[2,3], Jephté N'dri Koffi[1], Crystel Natacha Bohoussou[3]

[1]Félix Houphouët-Boigny University, Earth Science and Mining Resources Training and Research Unit (UFR STRM), University Center for Research and Application in Remote Sensing (CURAT), Abidjan, Côte d'Ivoire
[2]Félix Houphouët-Boigny University, Biosciences Training and Research Unit, Center for Research and Application in Remote Sensing (CURAT), Abidjan, Côte d'Ivoire
[3]Félix Houphouët-Boigny University, Biosciences Training and Research Unit (UFR Biosciences), Laboratory of Natural Environments and Biodiversity Conservation, Abidjan, Côte d'Ivoire
Email: *saintrodrigueaka@live.fr

How to cite this paper: Aka, K. S. R., Dibi, H. N., Koffi, J. N., & Bohoussou, C. N. (2022). Land Cover Dynamics and Assessment of the Impacts of Agricultural Pressures on Wetlands Based on Earth Observation Data: Case of the Azagny Ramsar Site in Southern Côte d'Ivoire. *Journal of Geoscience and Environment Protection, 10,* 43-61.
https://doi.org/10.4236/gep.2022.105004

Received: February 28, 2022
Accepted: May 21, 2022
Published: May 24, 2022

Abstract

The Azagny Ramsar site has been the scene of very strong agricultural pressures for several decades. In Côte d'Ivoire, management policies, previously developed and implemented in wetlands, remain very sensitive and vulnerable to environmental changes. It is to overcome these environmental management difficulties that this study was carried out to assess the impacts of mainly industrial agricultural activities on the wetland. To achieve this goal, we mapped the land use dynamics of the study area by a series of Landsat imagery from 1988, 2002, 2008, and 2019 and obtained 11 classes. The spatial analysis of the dynamics of land use from these images has shown that the increase in agricultural operations around the protected area has favored the reduction of several ecosystems of natural plant formations (forests, savannas, mangroves) amounting to 36.34% to the benefit of artificial plant formations such as rubber, oil palm and coconut trees (42.73%). However, these losses of natural plant formations are more accentuated outside the Ramsar site (peripheral zone) than in the Ramsar site with the example of mangroves which have lost 3.27% of their area in the Ramsar site against 33.80% in the peripheral zone between 1988 and 2019. These changes are less accentuated in the Ramsar site than on the periphery thanks to the vigilance of the Ivorian

Office of Parks and Reserve (OIPR) and natural barriers (watercourses) that surround it.

Keywords

Azagny, Ramsar, Land Use, Wetland, Agricultural Pressure, Ivory Coast

1. Introduction

Wetlands, the cradles of biodiversity and key constituent of our environment, are among the most productive ecosystems housing more or less all floral and faunal taxonomic units (Garg, 2015). Wetlands are recognized as one of the world's most valuable natural resources (Wu, 2018). They contain important animal species including birds, mammals, reptiles, amphibians, fish and plants including granaries of genetic material. As for example, water birds such as the whalers tern *Sternula balaenarum* and the Eurasian Curlew *Numenius arquata* (Ramsar Convention on Wetlands). Despite this importance, wetlands have fallen sharply worldwide. We notice that with the increasing world population, human demands on wetland resources for agricultural expansion and urban development continue to increase. In addition, due to climate change, coastal urban development, the last decades have seen significant decreases of ecologically and economically valuable coastal wetlands around the world (Chen et al., 2019; Gabler et al., 2017; Zhang et al., 2015). Wetlands are now more degraded and threatened by various anthropogenic pressures, including agricultural activities (Hu et al., 2020). In Côte d'Ivoire, the Ramsar site of Azagny encounters these same aggressions. These are mainly agricultural pressures. Through its actions to fight and protect national parks, the Ivorian Office of Parks and Reserves (OIPR) organizes each year inter-village competitions such as the Village Associations of Conservation and Development (AVCD) which allows local populations to participate in the protection of parks and reserves. In fact, Azagny is the first Ramsar site in Côte d'Ivoire since February 1996 and benefits from two protection statuses: that of a national park and a wetland of international importance. Given its importance in conservation in terms of the presence of biodiversity at the national and sub-regional level, many works have been carried out there (Koffi, 2016; Konan, 2008). But the manager of the site, the Ivorian Office of Park and Reserve (OIPR), does not have enough details on the land cover/use map of this protected area, even in the literature it is difficult to find it. Spatial control of space thus became a major concern for all authorities in charge of the environment especially for the Azagny's Ramsar site.

However, Azagny Ramsar site is hostile and heterogeneous in its ecosystem. As a result, Remote Sensing and Geographic Information Systems (GIS) are two tools that offer new perspectives for vegetation cover mapping. Indeed, Satellite images with different spatial and spectral resolutions and various analysis methods are effective techniques of quantifying changes in wetland (Shen, Yang, Jin, Xu, & Zhou, 2019; Toure, Stow, Shih, Weeks, & Lopez-Carr, 2018). Due to long record of continuous observation, spatial resolution and several observations, the Landsat series of satellite images have become one of the most essential data especially for dynamic monitoring of land use/cover (Hu et al., 2020), which have been widely used in forest degradation, wetland loss and assessment (Ajaj, Pradhan, Noori, & Jebur, 2017). But an effective wetland management and protection requires understanding the main causes and analyzing the process and trends of wetland changes. This is how "GMES and Africa" through its support program for environmental monitoring and security in partnership with the African Union initiated the GDZHAO project: "Sustainable Management of Wetlands for strengthening food security and ecosystem resilience in West Africa" which grouped eight (8) West African countries including Côte d'Ivoire through two (2) Ramsar sites. Through this study, we are going to discover spatially Azagny Ramsar site land use and its immediate environment under agricultural pressures by earth data observation. Especially, this article aims to contribute to better management of the Azagny Ramsar site by providing up-to-date spatial information on the dynamics of plant resources under the pressure of agricultural activities.

2. Materials and Methods

2.1. Study Area

The Azagny National Park, located in the south of Côte d'Ivoire, between 5˚14' and 5˚31' north latitude and 4˚76' and 5˚01' west longitude, covers an area of 21,850 ha. This Park is located in the "Lagoon Region", in the Ivorian coastal sector, about 125 km from Abidjan (**Figure 1**). It extends over the entire department of Grand-Lahou and Jacqueville and is part of the phytogeographical region of "Upper Guinea" which goes from Togo to Senegal (Gnagbo, 2017).

2.2. Materials

The materials used are composed of satellite and map data, software, and field equipment. In terms of satellite images, we used four (4) types of Landsat images from Earth explorer platform summarized in **Table 1** below:

The mapping data used include: a digital layer of the boundary of the Azagny Ramsar site produced and updated by the OIPR; vector layers from the OIPR database (the road network, the main hydrographic network, the site's facilities and equipment), all in shapefile extension. As for software, three (3) software programs made it possible to carry out this study. These are: ENVI 5.3; ArcGis 10.5; and Microsoft Excel. The field equipment used consisted mainly of Global Positioning System (GPS), cameras and notebook.

2.3. Methods

2.3.1. Pre-Processing of Satellite Images

This step consists in improving the radiometric, spectral and visual quality of the acquired images by reducing the atmospheric effects due to interactions with

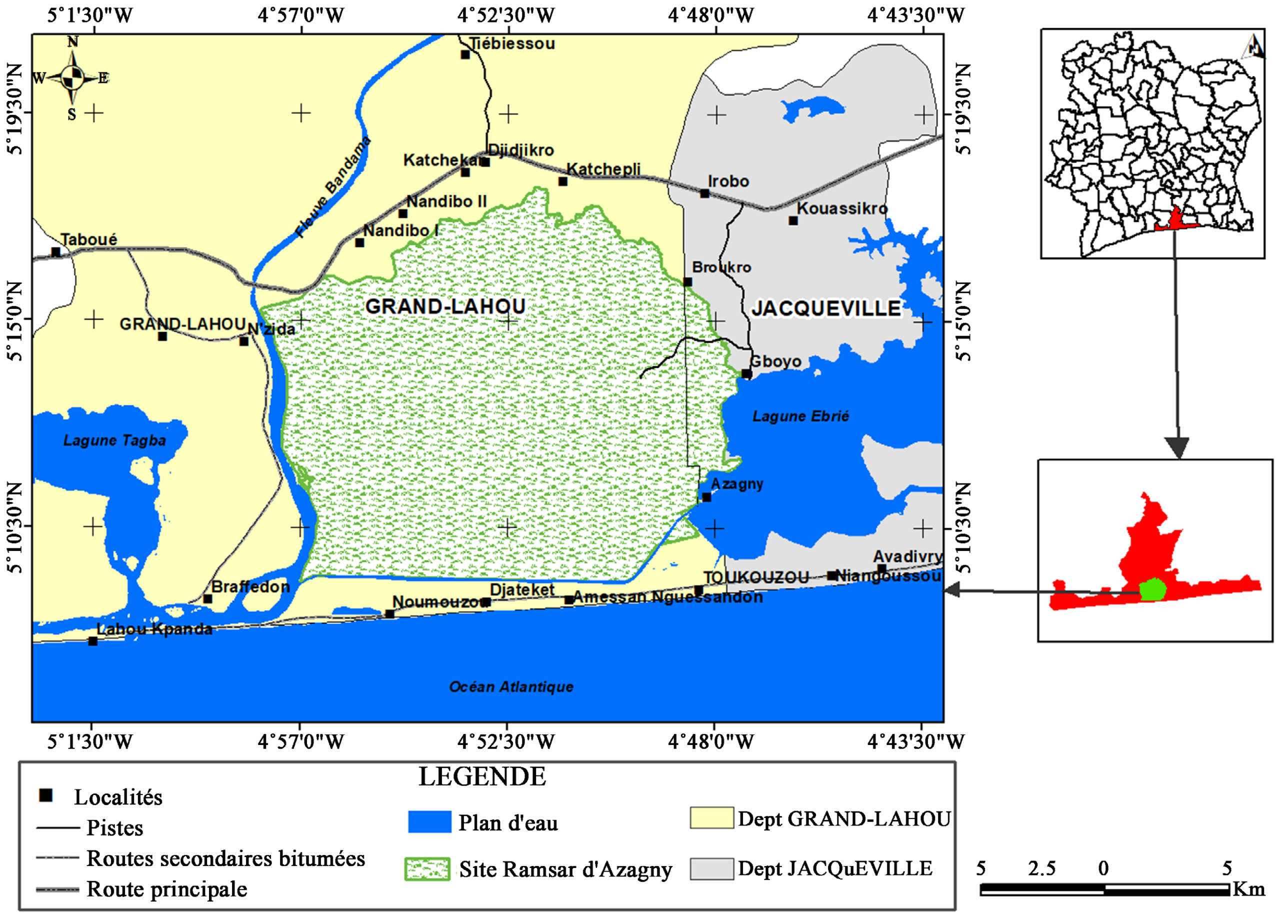

Figure 1. Geographical location of the Azagny Ramsar site.

Table 1. Acquisition date of Landsat images.

Images	Scenes (Path/Row)	Date of acquisition
Landsat Thematic Mapper (TM4) of 1988	196 - 56	24-12-1988
Landsat Enhanced Thematic Mapper (ETM+) of 2002	196 - 56	31-12-2002
Landsat Enhanced Thematic Mapper (ETM+) of 2008	196 - 56	30-01-2008
Landsat-8 Operational Land Imager (OLI) of 2019	196 - 56	20-01-2019

particles that cause disturbances in electromagnetic radiation. This manipulation was done from the Envi 5.3 software on all Landsat images and involves the sensor parameters during shooting. This is important because it improves visibility and enhances the spectral characteristics of the image.

2.3.2. Processing of Satellite Images

1) Index calculation

Satellite Image Processing consists of applying biophysical index calculations to images in order to highlight certain characteristics based on their reflectance. To do this, we calculated the Normalized Difference Vegetation Index (NDVI) on all 4 Landsat images into Envi 5.3 software in individual ways to highlight the vegetated surfaces. The NDVI formula is written as follows:

$$\mathrm{NDVI} = \frac{\mathrm{PIR} - \mathrm{R}}{\mathrm{PIR} + \mathrm{R}} \quad (1)$$

Then, index resulting from the Tasseled Cap transformation whose program is implemented and executable in the Envi 5.3 software were been calculated and applied to the Landsat images. These indexes are used to enhance the brightness of the images (Brightness Index) and to enhance the areas of humidity on the images (Water Index), Crist and Cicone (1984). Other neo-channels such as Principal Component Analysis (PCA) from the Envi 5.3 software have been created to facilitate the reading of information on Landsat images.

NDBI: (Normalized Difference Brightness Index):

$$\mathrm{NDBI} = \left(\mathrm{R}^2 + \mathrm{PIR}^2\right)^{1/2} \quad (2)$$

NDWI: (Normalized Difference Water Index):

$$\mathrm{NDWI} = \frac{\mathrm{PIR} - \mathrm{MIR}}{\mathrm{PIR} + \mathrm{MIR}} \quad (3)$$

2) RGB Colored

RGB colored uses three channels. According to Boussaada-Maabdi et al. (2017), it allows for better discrimination between geographical objects. For this study, the RGB colored chosen are those of the 4/8/10 bands for Landsat-8 (sample image) because they were the ones that showed better discrimination in the types of land use chosen. In feasibility, it was assigned respectively band 4 of the visible, band 8 of the near infrared and band 11 of the middle-infrared to the red (R), green (V) and blue (B) channels. These different RGB colored were made after the different indexes in order to better discriminate the units of land use to be characterized.

2.3.3. Choice of Sites to Visit

Thanks to the calculation and application of index and RGB colored made on the images, the different large entities namely, forests, savannahs, water, bare soils and habitats were identified. For the characterization of the land cover typology, the sites are selected in the Ramsar site and its peripheral area (**Figure 2**). 180 control points have been chosen in proportion to the areas of the different typologies of land cover present. The geographical coordinates of the points taken from the images are integrated into the GPS for the collection of field data.

2.3.4. Data Collection

The 05-day field mission made it possible to browse and verify the selected checkpoints upstream. On the ground, a careful observation of the different types of vegetation that litter the site was carried out. Indeed, it was a question of taking GPS points of the plant formations and all other land cover units visited, followed by descriptions and photos in support of these entities on the one hand and on the other hand to check and confirm the GPS points selected from the

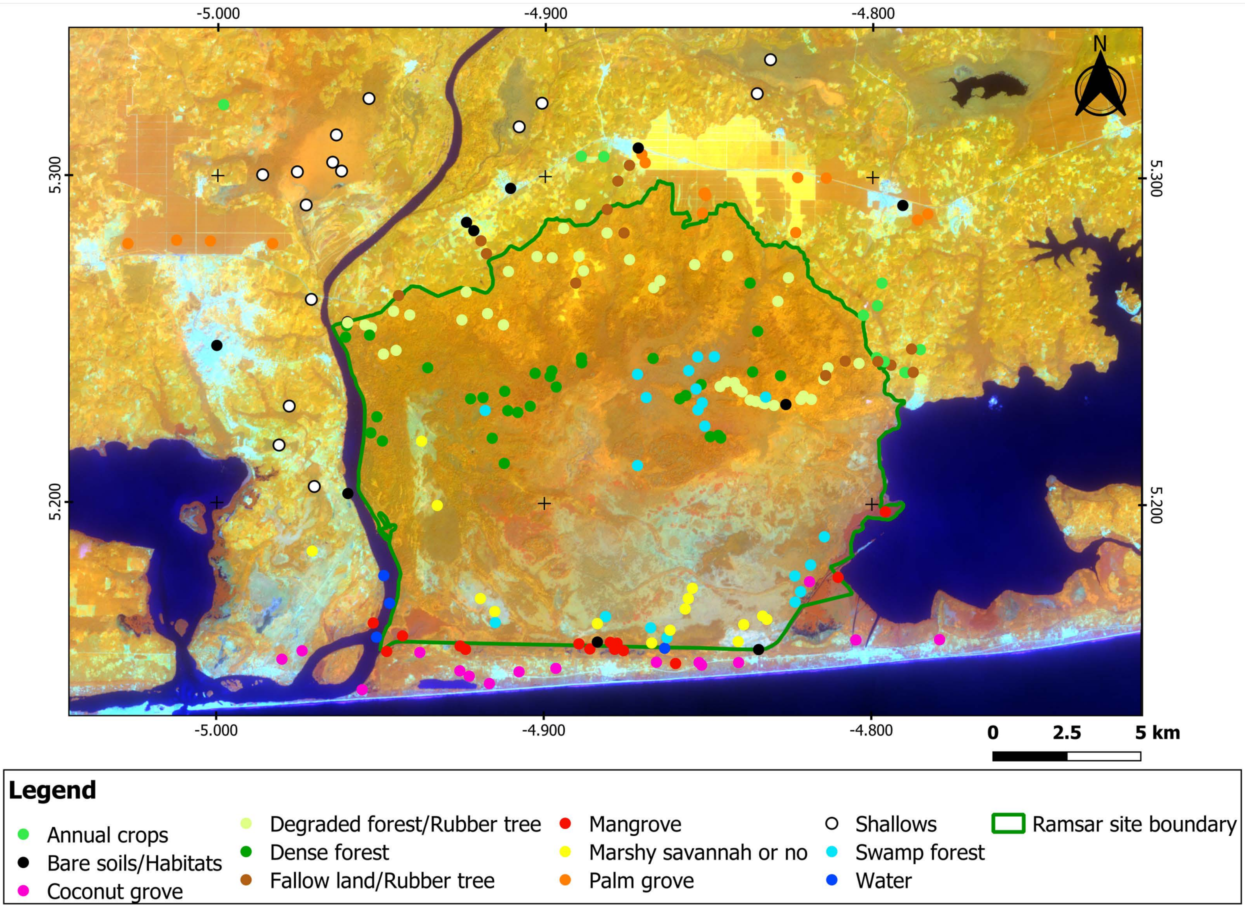

Figure 2. Map of distribution of sites to visit.

satellite image (Landsat-8).

2.3.5. Image Classification and Spatio-Temporal Dynamics of Land Cover

In order to achieve land cover dynamics, the most recent image (Landsat-8) was chosen as a sample image for classification. This classification was done in two stages: The first consisted in identifying the major groups of land use, namely: dense formations, sparsely dense formations, water surfaces, bare soils and habitat sites. The second step made it possible to extract the subunits by pixel-oriented classification by the maximum likelihood method (N'Da et al., 2008; Orimoloye et al., 2019) on the Landsat-8 image in the Envi 5.3 software.

These two stages of classifications made it possible to have a classified image in raster format and export in the ArcGis software for conversions in vector format (shapefile). This is how from step by step we obtained the land use classes with the Landsat-8 image. Indeed, with the reference image (Landsat-8) already classified, we obtain ROI (Region of Interest) which constitute training plot. These ROIs are then superimposed on each Landsat image and proceed by eliminating the training plots whose land use is no longer the same and the keep of those whose land use has remained the same. This process is done by analogy and respectively on the images of 2008, then 2002 and finally on that of 1988.

We then launch the classification and we obtain the desired classes.

2.3.6. Validation of Classifications

In order to validate the land cover classifications carried out, two (2) types of assessments were possible. The first is a visual comparative analysis of the basic RGB colored used for the classification and the land cover map carried out. When it looks similar between the two pieces of information produced, then the analysis can be validated. The second was devoted to assessing the overall performance level of each land cover classification by analysing the confusion matrices. According to Skupinski et al. (2009), the Kappa index characterizes the ratio of well-ranked pixels to total pixels surveyed. The confusion matrix is as follows: the rows represent the assignment of pixels to each theme after classification; the columns indicate the actual distribution of pixels in each theme; and the diagonal represents the percentages of well-ranked pixels.

2.3.7. Assessment of the Dynamics of Agricultural Pressure on the Ramsar Site and Its Peripheral Area

1) Assessment of land cover dynamics by the transition matrix

The analysis of the changes that occurred over the entire study period was done by the four Landsat images. It produces a change detection matrix from the comparison between the maps of the two dates Girard and Girard (1999). Subsequently, the global rate of change (Tg) of spatial expansion was calculated.

2) Analysis of the rate of change of land use units

The Overall Change Rate (Tg) is used to estimate the overall progress (the proportion of gain or loss) of the areas of land use units. It was calculated to specifically assess the pressure of farms on the Azagny Ramsar site between 1988 and 2019. The overall rate of change is obtained from the following mathematical formula:

$$Tg = \left[\left(S_2 - S_1\right)/S_1\right] \times 100$$

where:

Tg = Overall rate of change (%);

S_1 = Area of the class on date t_1 (initial date);

S_2 = Area of the class on the date t_2 (final date), and $t_2 > t_1$.

Analysis of the values of the rate of change shows that the positive values indicate a “progression” and the negative values indicate a “regression”. Values close to zero indicate that the class remains relatively “stable”.

3. Results

3.1. Mapping of the Spatio-Temporal Dynamics of Land Cover of the Azagny Ramsar Site and Its Peripheral Area

3.1.1. Evolution of Land Cover Areas

For each Landsat image processed, we obtained eleven (11) classes namely: DF = degraded forest; DFTF = dense forest temporarily flooded; SW = swamp forest, CSSN = coastal savannah swampy or no; FMPCRC = fallow mosaic perennial crops dominated by rubber and coconut; FMPCOP = fallow mosaic perennial crops dominated by oil palm; MFAC = mosaic fallow annual crops; MSH = marshy shallows with herbaceous; M = mangrove; PE = water body and BSH = bare soils and habitats. Table 2 below shows superficies dynamics in hectare of each unit of land use from 1998 to 2019.

This evolution of land use typologies is very unequal. Figure 3 shows graphically the evolution of the different types of land use.

3.1.2. Analysis of Confusion Matrices

The overall cartographic accuracy of the different classification treatments on the images of 1988, 2002, 2008 and 2019 are respectively 82.42%; 84.62%; 85.42%

Table 2. Evolution of land cover areas from 1988 to 2019.

Land use	1988	2002	2008	2019
DF	5873.22	7572.148	7713.061	5342.669
DFTF	8712.099	3136.288	3442.6	5088.987
SW	8453.476	10844.396	10170.649	9073.341
CSSN	8933.903	6107.61	6089.216	6018.292
BSH	2022.66	3358.703	3285.231	3988.817
M	1957.003	966.44	738.892	895.204
MFAC	6710.145	5908.616	4951.455	2669.669
FMPCRC	20167.143	23133.159	24302.292	28805.562
FMPCOP	4288.676	6269.975	6525.573	6633.642
MSH	3524.027	3802.11	3624.49	2065.861
WB	18881.007	18423.914	18679.9	18941.315
TOTAL	**89523.359**	**89523.359**	**89523.359**	**89523.359**

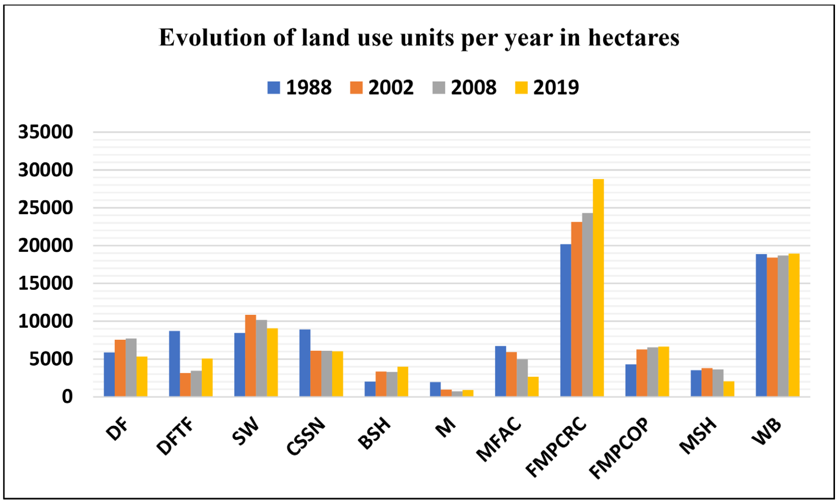

Figure 3. Spatial-temporal evolution of areas in Hectares (Ha) of land use types from 1988 to 2019.

and 88.21% (Tables 3-6). For all these treatments, the most important confusions are observed between swamp forest classes and temporarily flooded dense forests and mangroves. Other equally important confusions are observed between the class Mosaic rubber and coconut grove and the classes degraded forest, then the

Table 3. Confusion matrix of the 1988 Landsat TM image classification.

Data Classified	DF	DFTF	SW	CSSN	FMPCRC	FMPCOP	MFAC	MSH	M	WB	BSH	Row Total
DF	**94.55**	1.04	0.81	0.00	1.75	5.00	0.00	0.00	0.00	0.00	0.00	**103.15**
DFTF	2.73	**94.81**	2.42	0.00	0.00	0.00	0.00	0.00	0.00	0.00	0.00	**99.95**
SW	0.00	2.86	**93.55**	0.00	0.00	6.25	0.00	0.00	0.00	0.00	0.00	**102.66**
CSSN	0.00	0.65	1.61	**92.59**	0.00	0.00	2.78	6.67	0.00	0.00	11.11	**115.41**
FMPCRC	2.73	0.65	0.81	1.85	**91.23**	6.25	0.00	0.00	0.00	0.00	5.56	**109.07**
FMPCOP	0.00	0.00	0.00	0.00	1.75	**75.00**	2.78	0.00	0.00	0.00	0.00	**79.53**
MFAC	0.00	0.00	0.00	1.85	1.75	1.25	**88.89**	0.00	0.00	0.00	5.56	**99.30**
MSH	0.00	0.00	0.00	0.00	1.75	0.00	5.56	**86.67**	0.00	0.00	0.00	**93.98**
M	0.00	0.00	0.81	0.00	0.00	6.25	0.00	6.67	**100.0**	0.00	0.00	**113.72**
WB	0.00	0.00	0.00	0.00	0.00	0.00	0.00	0.00	0.00	**100.0**	0.00	**100.00**
BSH	0.00	0.00	0.00	3.70	1.75	0.00	0.00	0.00	0.00	0.00	**77.78**	**83.24**
Column Total	**100**	**100**	**100**	**100**	**100**	**100**	**100**	**100**	**100**	**100**	**100**	**1100**

Overall accuracy = 82.42%; Kappa = 0.89. DF = degraded forest; DFTF = dense forest temporarily flooded; SW = swamp forest, CSSN = coastal savannah swampy or no; FMPCRC = fallow mosaic perennial crops dominated by rubber and coconut; FMPCOP = fallow mosaic perennial crops dominated by oil palm; MFAC = mosaic fallow annual crops; MSH = marshy shallows with herbaceous; M = mangrove; PE = water body; BSH = bare soils and habitats.

Table 4. 2002 Landsat ETM+ image classification confusion matrix.

Data Classified	DF	DFTF	SW	CSSN	FMPCRC	FMPCOP	MFAC	MSH	M	WB	BSH	Row Total
DF	**92.73**	0.65	0.81	0.00	2.63	6.25	0.00	0.00	0.00	0.00	0.00	**103.06**
DFTF	1.82	**94.81**	3.23	0.00	0.00	0.00	0.00	0.00	0.00	0.00	0.00	**99.85**
SW	1.82	3.25	**93.55**	0.00	0.00	3.13	0.00	0.00	7.69	0.00	0.00	**109.43**
CSSN	0.00	0.00	0.81	**96.30**	0.00	0.00	0.00	0.00	0.00	0.00	2.78	**99.88**
FMPCRC	1.82	1.30	0.00	0.00	**94.74**	3.13	4.44	0.00	0.00	0.00	2.78	**108.20**
FMPCOP	0.00	0.00	0.81	0.00	0.00	**81.25**	3.89	0.00	0.00	0.00	0.00	**85.95**
MFAC	1.82	0.00	0.00	0.00	1.75	3.13	**83.33**	0.00	0.00	0.00	0.00	**90.03**
MSH	0.00	0.00	0.00	0.00	0.00	3.13	8.33	**86.67**	0.00	0.00	0.00	**98.13**
M	0.00	0.00	0.81	0.00	0.00	0.00	0.00	6.67	**92**	0.00	0.00	**99.78**
WB	0.00	0.00	0.00	0.00	0.00	0.00	0.00	3.33	0.00	**100**	0.00	**103.33**
BSH	0.00	0.00	0.00	3.70	0.88	0.00	0.00	3.33	0.00	0.00	**94.44**	**102.36**
Column Total	**100**	**100**	**100**	**100**	**100**	**100**	**100**	**100**	**100**	**100**	**100**	**1100**

Overall accuracy = 84.62%; Kappa = 0.91.

Table 5. 2008 Landsat ETM+ image classification confusion matrix.

Data Classified	DF	DFTF	SW	CSSN	FMPCRC	FMPCOP	MFAC	MSH	M	WB	BSH	Row Total
DF	**90.91**	1.95	0.81	1.48	2.63	3.13	1.11	0.00	0.00	0.00	0.00	**102.01**
DFTF	1.45	**94.81**	3.23	0.00	0.00	0.00	0.00	0.00	1.54	0.00	0.00	**101.02**
SW	0.00	1.95	**93.55**	0.00	0.00	3.13	0.00	6.67	2.31	0.00	0.00	**107.60**
CSSN	0.00	0.00	0.81	**92.59**	0.00	0.00	0.00	0.00	0.00	0.00	0.00	**93.40**
FMPCRC	2.73	0.39	0.81	0.00	**94.74**	3.13	2.78	0.00	0.00	0.00	2.78	**107.34**
FMPCOP	3.27	0.26	0.00	0.00	0.88	**87.50**	0.00	0.00	3.08	0.00	1.67	**96.65**
MFAC	0.55	0.39	0.00	0.00	0.88	0.00	**94.44**	0.00	0.00	0.00	0.00	**96.26**
MSH	0.36	0.00	0.00	2.96	0.00	0.00	1.67	**80.00**	0.00	0.00	1.11	**86.10**
M	0.00	0.26	0.81	0.00	0.00	3.13	0.00	6.67	**92.31**	0.00	0.00	**103.17**
WB	0.73	0.00	0.00	0.00	0.00	0.00	0.00	0.00	0.77	**100.0**	0.00	**101.50**
BSH	0.00	0.00	0.00	2.96	0.88	0.00	0.00	6.67	0.00	0.00	**94.44**	**104.95**
Column Total	**100**	**100**	**100**	**100**	**100**	**100**	**100**	**100**	**100**	**100**	**100**	**1100**

Overall accuracy = 85.42%; Kappa = 0.91.

Table 6. 2019 Landsat OLI image classification confusion matrix.

Data Classified	DF	DFTF	SW	CSSN	FMPCRC	FMPCOP	MFAC	MSH	M	WB	BSH	Row Total
DF	**94.55**	1.69	0.81	0.00	2.24	0.00	1.67	0.00	0.00	0.00	0.00	**100.95**
DFTF	2.18	**94.81**	2.90	0.00	0.34	0.00	0.00	0.00	5.38	0.00	0.00	**105.62**
SW	0.91	3.12	**95.16**	0.00	0.00	1.88	0.00	0.00	0.00	0.00	0.00	**101.06**
CSSN	0.91	0.13	0.32	**96.15**	0.00	0.00	0.00	1.33	0.00	0.00	4.44	**103.29**
FMPCRC	0.91	0.26	0.00	1.15	**96.55**	3.13	2.78	0.00	0.00	0.00	1.11	**105.89**
FMPCOP	0.00	0.00	0.00	0.00	0.00	**93.75**	2.78	0.00	0.00	0.00	0.00	**96.53**
MFAC	0.55	0.00	0.00	0.00	0.52	0.00	**88.89**	2.00	0.00	0.00	0.00	**91.95**
MSH	0.00	0.00	0.00	1.92	0.00	0.00	2.78	**93.33**	3.85	0.00	0.00	**101.88**
M	0.00	0.00	0.81	0.00	0.00	1.25	0.00	3.33	**84.62**	0.00	0.00	**90.01**
WB	0.00	0.00	0.00	0.00	0.00	0.00	0.00	0.00	6.15	**100**	0.00	**106.15**
BSH	0.00	0.00	0.00	0.77	0.34	0.00	1.11	0.00	0.00	0.00	**94.44**	**96.67**
Column Total	**100**	**100**	**100**	**100**	**100**	**100**	**100**	**100**	**100**	**100**	**100**	**1100**

Overall accuracy = 88.21%; Kappa = 0.93. DF = degraded forest; DFTF = dense forest temporarily flooded; SW = swamp forest, CSSN = coastal savannah swampy or no; FMPCRC = fallow mosaic perennial crops dominated by rubber and coconut; FMPCOP = fallow mosaic perennial crops dominated by oil palm; MFAC = mosaic fallow annual crops; MSH = marshy shallows with herbaceous; M = mangrove; WB = water body; BSH = bare soils and habitats.

class bare soil/Habitat and coastal savannah. Apart from these three cases, all other types of land use are relatively well discriminated against.

3.1.3. Quantitative and Qualitative Analysis of Classification Dynamics

The land cover maps of the study area for the years 1988, 2002, 2008 and 2019 are shown in Figures 4-7. The central part of the study area is occupied by the

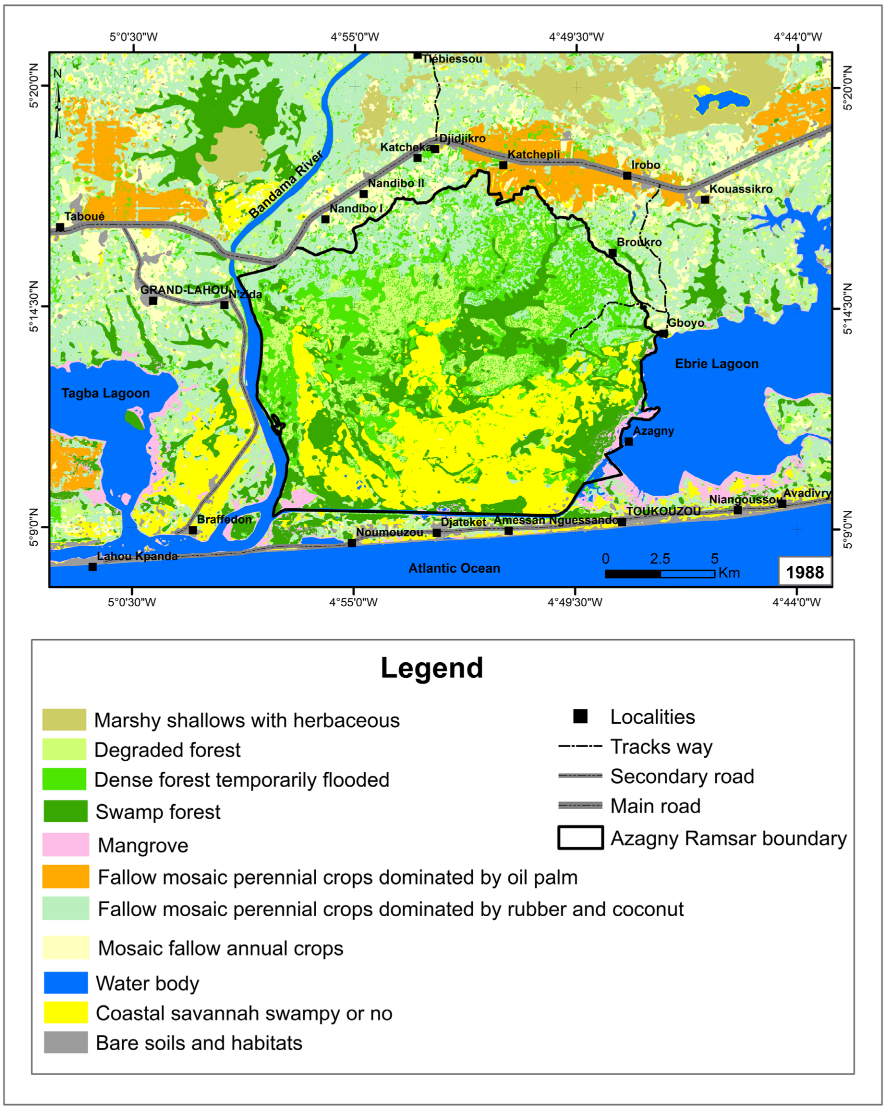

Figure 4. Azagny Ramsar land use in 1988 from Landsat images.

Ramsar site. At the qualitative level, it is observed that the latter is mainly covered with natural plant formations (forest, savannah and mangrove). Unlike the area within the Ramsar site, the peripheral area is covered by agricultural holdings. Thus, the outer lands of the Ramsar site are occupied by large plots of palm oil and rubber, while the coastal area is rather dominated by coconut groves. Some mangrove islets are also in the peripheral area. At the quantitative level, we are observing:

- A gradual decrease in the areas of temporarily flooded dense forests (DFTF) from 8712.099 to 5088.987 ha;
- A drastic decrease in mangroves (M) from 1988 to 2019 (from 1957.003 to 895.204 ha);
- A decrease in the area of coastal savannahs swampy or no (CSSN) from 1988 to 2002 (8933.903 to 6107.61 ha);
- A decrease in mosaic areas fallow annual crops (MFAC) from 1988 to 2019 (6710.145 to 2669.669 ha);

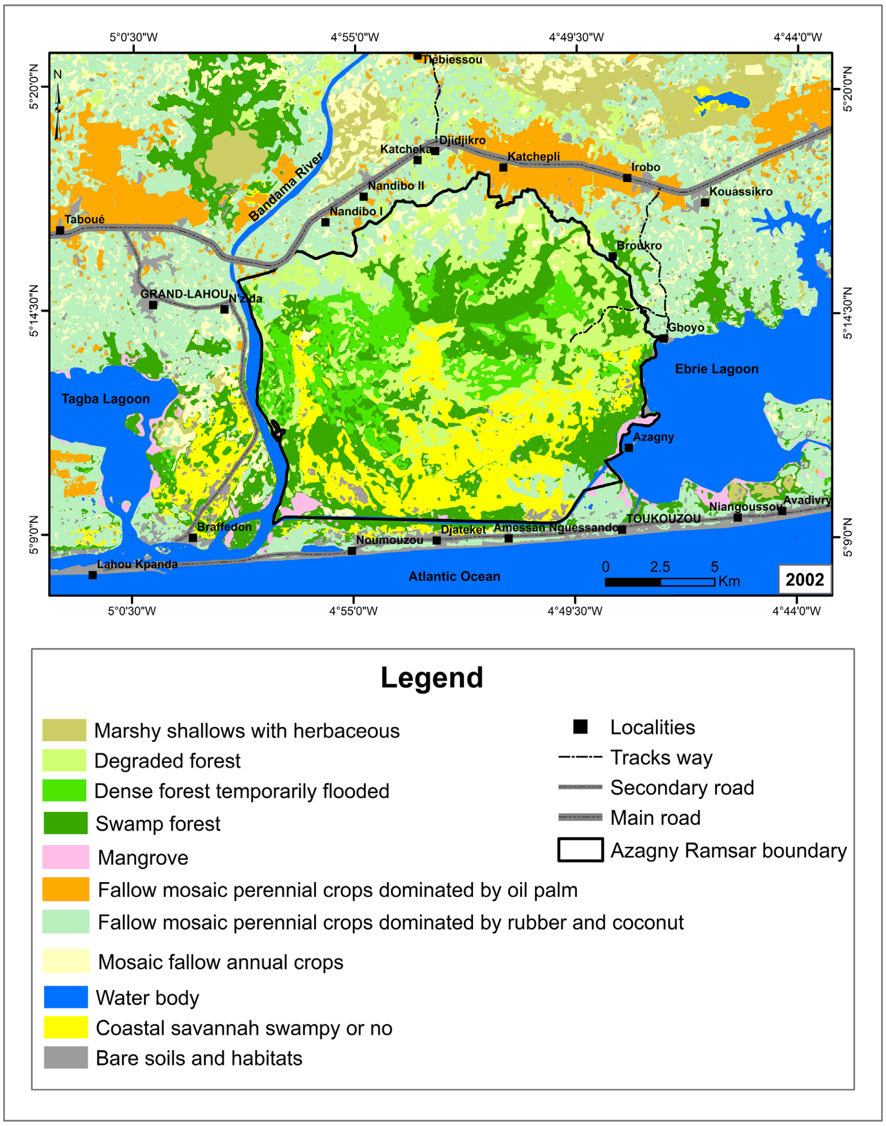

Figure 5. Azagny Ramsar land use in 2002 from Landsat images.

- An increase in mosaic areas fallow perennial crops dominated by rubber and coconut (FMPCRC) from 1988 to 2019. (From 20167.143 to 28805.562 ha);
- A slight but gradual increase in fallow mosaics perennial crops dominated by oil palm (FMPCOP) from 2002 to 2019 from 6269.975 to 6633.642 ha;
- An increase in bare soils and habitat sites from 2022.66 Ha in 1988 to 3988.817 Ha in 2019.

These spatio-temporal dynamics of the land cover units observed quantitatively are assessed upstream by Table 2 including the areas in hectares (Ha).

3.2. Assessment of the Dynamics of Agricultural Pressures on the Ramsar Site and Its Peripheral Area

3.2.1. Assessment of the Dynamics of Agricultural Pressures by the Transition Matrix

The analysis of changes over the entire study period was highlighted by transition

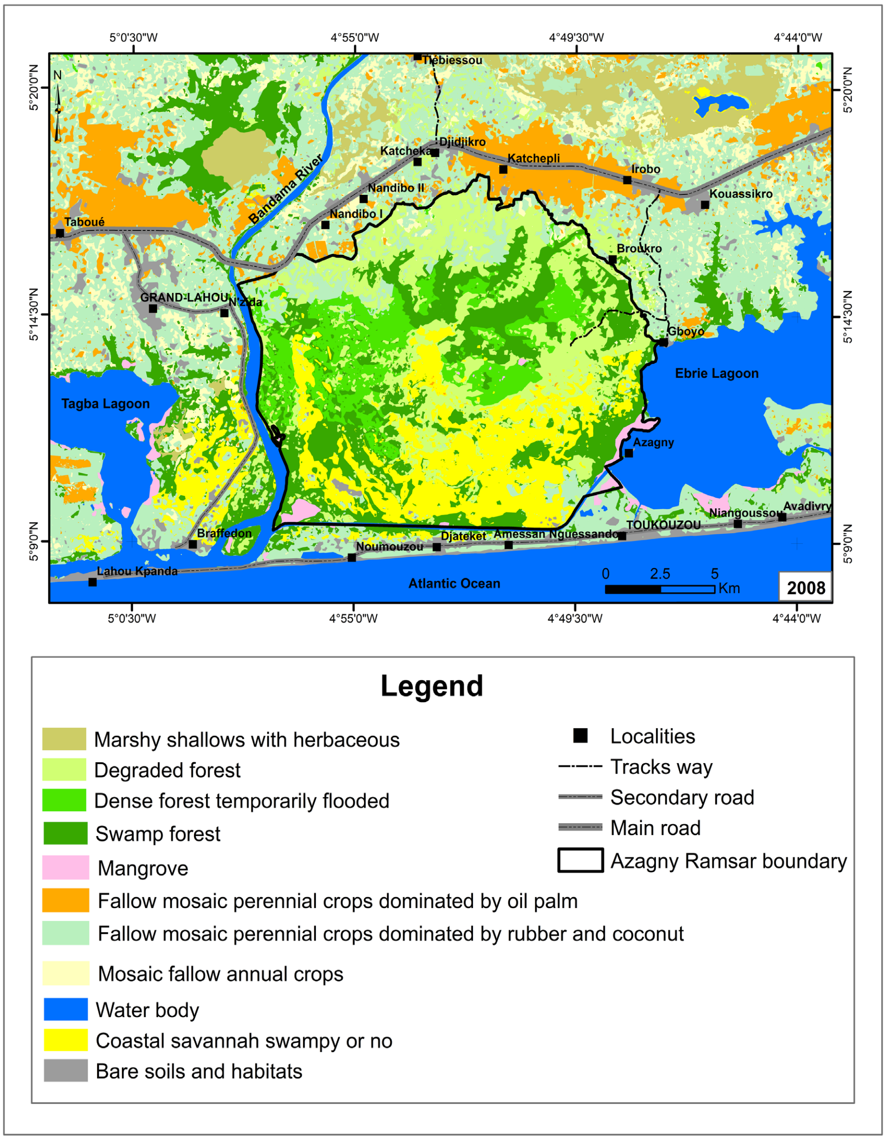

Figure 6. Azagny Ramsar land use in 2008 from Landsat images.

matrices. Changes across the whole study area, inside and outside of the Ramsar site (Global, Inside, Peripheral) were determined. These changes are determined between four periods: 1988-2002; 2002-2018; 2008-2019 and 1988-2019. In sum, twelve (12) transition matrix were generated. We have therefore noted through this assessment that natural plant formations [(DF = degraded forest; DFTF = dense forest temporarily flooded; SW = swamp forest, CSSN = coastal savannah swampy or no; MSH = marshy shallows with herbaceous; M = mangrove)] decrease to leave place for perennial crops [(rubber trees, oil palms and coconut trees)] through this figure (Figure 8).

These observed mutations are losses of natural plant formations expressed in percentages (%) during the 4 periods mentioned.

In detail, Figure 9 and Figure 10 below show the peripheric zone and Ramsar site mutations carried out respectively.

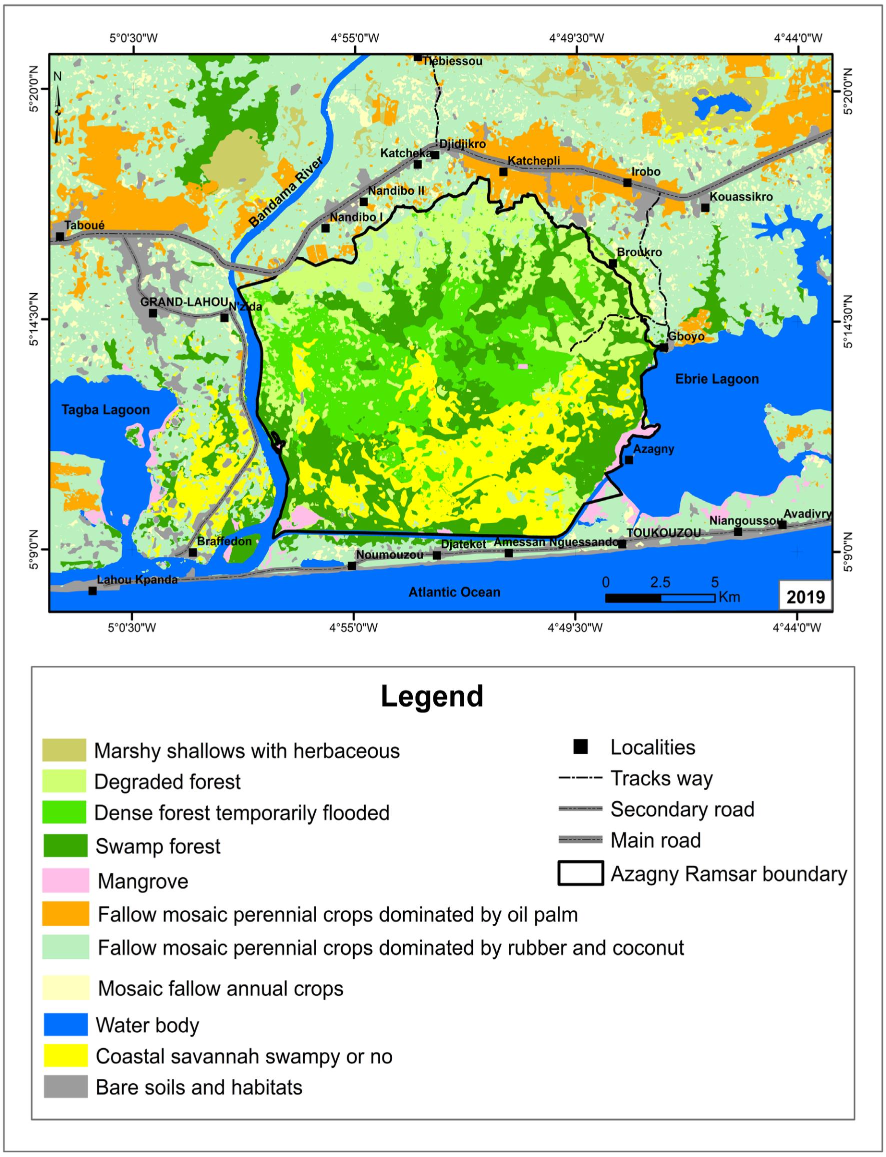

Figure 7. Azagny Ramsar land use in 2019 from Landsat images.

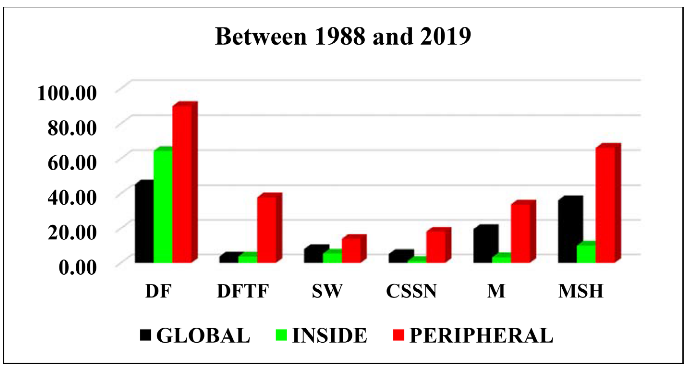

Figure 8. Losses of natural plant formations in percentage (%) between 1988 and 2019.

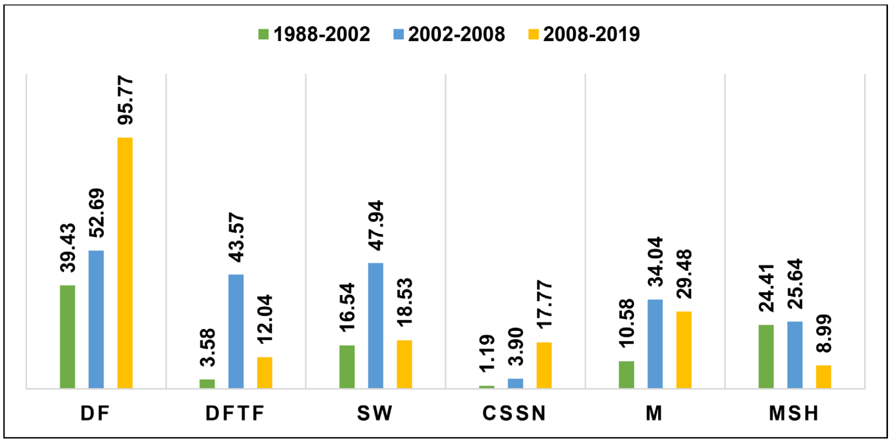

Figure 9. Losses of natural plant formations (%) in the peripheral zone.

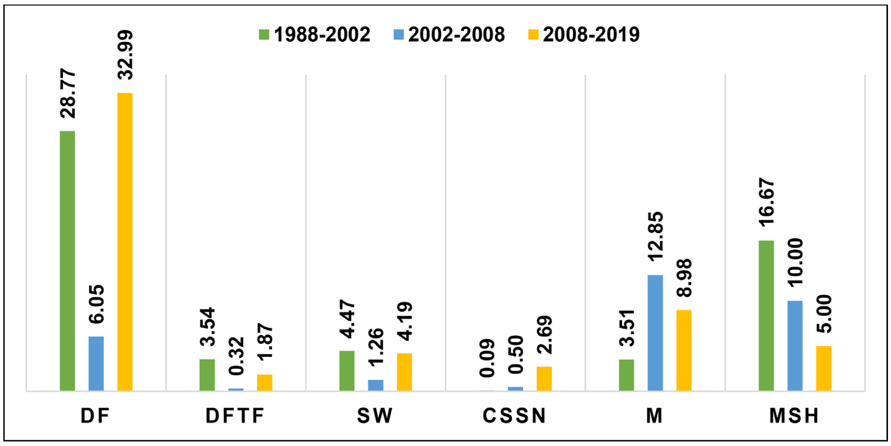

Figure 10. Losses of natural plant formations (%) in the Ramsar site.

3.2.2. Assessment of the Dynamics of Agricultural Pressures by the Overall Rate of Change

The overall rate of change made it possible to estimate the overall increase (the proportion of gain, stability or loss) of surface areas of land use units. Analysis of the values of the rate of change shows that the positive values indicate a "progression" and the negative values indicate a "regression". Values close to zero indicate that the class remains relatively "stable". Also, from one period to another, some classes have gradually declined to the detriment of other land use units (Figure 11).

4. Discussion

4.1. Spatio-Temporal Dynamics of Land Cover

The Analysis of the spatio-temporal dynamics of land cover at the Azagny Ramsar site made it possible to categorize 11 land use classes. The accuracy obtained during the treatments is 82.42% for the TM 1988 image, then 84.62% for ETM+ 2002; 85.42% for ETM+ 2008 and finally 88.21% for OLI 2019. These results are close to those obtained by Konan (2008), and Koffi (2016), who also worked on the same site. Noted that the methodology used for these classifications is that of

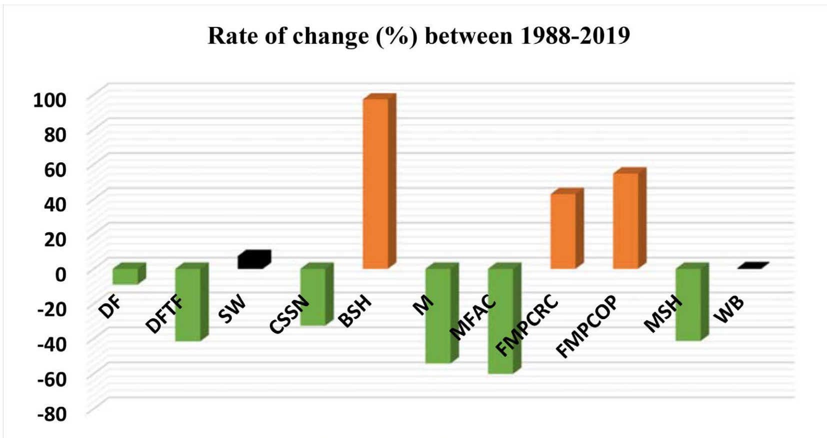

Classes of DF = degraded forest; DFTF = dense forest temporarily flooded; CSSN = coastal savannah swampy or no; MFAC = mosaic fallow annual crops; MSH = marshy shallows with herbaceous and M = mangrove experienced a regression during these years; The classes of SW = swamp forest and WB = water body, have remained relatively stable; The classes of FMPCRC = mosaic fallow perennial crops dominated by rubber and coconut; FMPCOP = mosaic fallow perennial oil palm-dominated crops; and BSH = bare soils and habitats experienced an increase during these periods.

Figure 11. Overall rate of change in the study area between 1998 and 2019.

the supervised oriented classification pixel by the probability method. This widely used approach is recognized for its performance in the detection, identification and characterization of spatial units. According to Mondal et al. (2012), it is one of the best known and most widely used classification algorithms in remote sensing. It is considered a basic method of pixels or a pixel is assigned to the class that has the maximum likelihood (maximum probability). According to Koffi (2016), this mapping method is based on the reflectance of objects from satellite images to identify and map the main types of land use. In addition, it should be noted that of the four Landsat images, the one that recorded the lowest cartographic accuracy was that of the TM sensor acquired in 1988. This would come from the great confusion recorded between the classes of swamp forests, temporarily flooded dense forest and mangrove on the one hand, then on the other hand the classes of fallow/perennial crops dominated by rubber and coconut and degraded forests, and finally the class coastal savannah swampy or no and bare soils and habitats. At that time, there were still significant forest covers in the rural area, so the fallow mosaics/perennial crops were mostly covered by relatively dense old fallow land which is why the confusion with degraded forests. As for the confusion savannahs and bare soil and habitats, it is explained by the fact that at that time the savannahs were constantly burned for hunting and therefore they take the reflectance of bare soils.

4.2. Analysis of the Impacts of Agricultural Holdings on the Ramsar Site

The decline in natural plant formations can be explained by the expansion of agricultural activities dominated by perennial crops. Fundamentally, the populations of these localities are for fishermen, but through the advance of agro-industrial industries such as Oil Palm industry Côte d'Ivoire (PALMCI), African Rubber Plantation Company (SAPH), in the area, the populations have become farmers (Resident). Bare soil and habitats classes and perennial crops increased sharply between 1988 and 2019. According to (Hu et al., 2020; N'Da et al., 2008), deforestation is strongly correlated with population growth. The search for new fertilize land for crops and suitable places for habitat strongly affects natural areas (Park, Ramsar site). In addition, one of the important remarks is the constant regression of the annual crops in the study area in favor of perennial crops. Between 1988 and 2002 according to the transition matrix, only 15.92% of the areas dedicated to annual crops remained stable and 54.96% of these areas were converted into perennial crops. This situation could lead to a food safety problem in the departments of Grand-Lahou and Jacqueville in the future. Finally, it is noted, at the level of land cover, that the year 2019 has less land covered by natural vegetation than the other dates, which further justifies that the Azagny Ramsar site is highly exposed by pressure from farms.

5. Conclusion

The analysis of Landsat satellite images (TM of 1988, ETM+ of 2002, 2008 and OLI of 2019) made it possible to assess the spatio-temporal dynamics of land use and to quantify the pressure of the impacts of perennial crops at the Azagny Ramsar site. Eleven (11) classes have been determined; these are: Degraded Forest, dense forest temporarily flooded, Swamp forest, Coastal Savannah swampy or no, Bare soils/Habitats, Mangrove, Fallow mosaic/annual crops, Fallow mosaic/perennial crops dominated by rubber and coconut, Mosaïque fallow/perennial crops dominated by oil palm, Marshy lowland with herbaceous, Water Body (Lagoon, River, Canal and Atlantic Ocean). This study shows that natural plant formations such as Forests, Savannahs and Mangroves have declined in favour of anthropized plant formations (rubber, coconut and oil palm). These losses amount to 42.73% for natural plant formations against 36.34% for artificial plant formations. This decrease in land cover units is all the more pronounced on the periphery than within the Ramsar site.

Azagny Ramsar site is a fragile environment but abounds various ecosystems. Therefore, monitoring with a high spatial resolution satellite image such as sentinel-2 would be greatly appreciated to better see the details of these land cover units. Then, 3/4 of its area is practically in the water. Only 1/4 is present on dry land. This study could have included a section for monitoring the water surfaces of the Ramsar site in order to see the evolution and the level of the waters according to the rainy or dry seasons. This is one of the shortcomings. Other insufficient observation of this study is the absence of a socio-economic survey of the local populations to find out why they enter in the site for activities knowing that it is proscribed. As a perspective in view of all these shortcomings, we plan to conduct studies on the seasonal dynamics of water surfaces using Radar images (drone data could be used to collect field data); Then, determine the quality of the waters of the Ramsar site with a view to assessing the level of pollution by the agricultural inputs used in the peripheral zone; Ultimately, analyze the perception of local residents on the use of products from the Ramsar site, and manage the site through more detailed land use mapping with Sentinel-2.

Acknowledgements

This study, especially this article, was made possible thanks to Dr DIBI N'Da Hyppolite, my Research Director and his entire team, in particular KOFFI N'Dri Jephté and BOHOUSSOU Natacha Crystel, whom I would like to thank. I would like to thank Professor KOUAME Koffi Fernand and Dr AKPA You Lucette from CURAT for their commitment and dedication during the execution of the GDZHAO project from which this study stems. I would like to thank Mr. AZANI Dede who was my internship supervisor during this period, Mr. BAKAYOKO, Hillihase, Mr. KOUAME N'dri Pascal, and Mr. WAMIEN Binger, all from the Ivorian Office of Parks and Reserves.

Conflicts of Interest

The authors declare no conflicts of interest regarding the publication of this paper.

References

Ajaj, Q. M., Pradhan, B., Noori, A. M., & Jebur, M. N. (2017). Spatial Monitoring of Desertification Extent in Western Iraq Using Landsat Images and GIS. *Land Degradation & Development, 28,* 2418-2431. https://doi.org/10.1002/ldr.2775

Boussaada-Maabdi, N., Bousnoubra-Kherici, H., Kherici, N., & Hammad, N. (2017). Mapping of Land-Cover from Remotely Sensed Images in the Valley of Oued Righ (Algerian Southeast). *Journal of Fundamental and Applied Sciences, 9,* 696-712. https://doi.org/10.4314/jfas.v9i2.6

Chen, H. W., Lin, H. C., Chuang, Y. H., Sun, C. T., Chen, W. Y., & Kao, C. Y. (2019). Effects of Environmental Factors on Benthic Species in a Coastal Wetland by Redundancy Analysis. *Ocean and Coastal Management, 169,* 37-49. https://doi.org/10.1016/j.ocecoaman.2018.12.003

Crist E. P., & Cicone, R. C. (1984). *Application of the Tasseled Cap Concept to Simulated Thematic Mapper Data* (10 p). Environmental Research Institute of Michigan.

Gabler, C. A., Osland, M. J., Grace, J. B., Stagg, C. L., Day, R. H., Hartley, S. B., & McLeod, J. L. (2017). Macroclimatic Change Expected to Transform Coastal Wetland Ecosystems This Century. *Nature Climate Change, 7,* 142-147. https://doi.org/10.1038/nclimate3203

Garg, J. K. (2015). Wetland Assessment, Monitoring and Management in India Using Geospatial Techniques. *Journal of Environmental Management, 148,* 112-123. https://doi.org/10.1016/j.jenvman.2013.12.018

Girard, M. C., & Girard, C. M. (1999). Traitement des Données de Télédétection (529 p). Dunod.

Gnagbo, A. (2017). Forest Dynamic after Abandoning Cocoa Farming in the Azagny National Park (Southern Côte d'Ivoire). *Global Journal of Advanced Research, 4,* 1-12. https://www.researchgate.net/publication/316741128

Hu, T., Liu, J., Zheng, G., Zhang, D., & Huang, K. (2020). Evaluation of Historical and Future Wetland Degradation Using Remote Sensing Imagery and Land Use Modeling. *Land Degradation and Development, 31,* 65-80. https://doi.org/10.1002/ldr.3429

Koffi, K. A. (2016). *Dynamique de la végétation et valeurs de conservation des espaces anciennement cultivés du parc national d'Azagny (sud de la Côte d'Ivoire)* (185 p). Thèse Doctorat, UFR Biosciences, Université Félix Houphouët-Boigny.

Konan K. E. (2008). Conservation de la diversité végétale et activités humaines dans les aires protégées du sud forestier ivoirien: L'exemple du Parc National d'Azagny (269 p). Thèse de Doctorat, Université de Cocody, Côte d'Ivoire.

Mondal, A., Kundu, S., Chandniha, S. K., Shukla, R., & Mishra, P. (2012). Comparison of Support Vector Machine and Maximum Likelihood Classification Technique Using Satellite Imagery. *International Journal of Remote Sensing and GIS, 1,* 116-123.

N'Da, D. H., N'guessan, K. E., Waddja, E. M., & Affian, K. (2008). Apport de la télédétection au suivi de la déforestation dans le Parc National de la Marahoué (Côte d'Ivoire). *Télédétection, 8,* 17-34.

Orimoloye, I. R., Mazinyo, S. P., Kalumba, A. M., Nel, W., Adigun, A. I., & Ololade, O. O. (2019). Wetland Shift Monitoring Using Remote Sensing and GIS Techniques: Landscape Dynamics and Its Implications on Isimangaliso Wetland Park, South Africa. *Earth Science Informatics, 12,* 553-563. https://doi.org/10.1007/s12145-019-00400-4

Shen, G., Yang, X., Jin, Y., Xu, B., & Zhou, Q. (2019). Remote sensing and evaluation of the wetland ecological degradation process of the Zoige Plateau Wetland in China. *Ecological Indicators, 104,* 48-58. https://doi.org/10.1016/j.ecolind.2019.04.063

Skupinski, G., Binh Tran, D., & Weber, C. (2009). Les images satellites Spot multi-dates et la métrique spatiale dans l'étude du changement urbain et suburbain—Le cas de la basse vallée de la Bruche (Bas-Rhin, France). *Cybergeo: European Journal of Geography, 439,* 95 p.

Toure, S. I., Stow, D. A., Shih, H. C., Weeks, J., & Lopez-Carr, D. (2018). Land Cover and Land Use Change Analysis Using Multi-Spatial Resolution Data and Object-Based Image Analysis. *Remote Sensing of Environment, 210,* 259-268. https://doi.org/10.1016/j.rse.2018.03.023

Wu, Q. (2018). GIS and Remote Sensing Applications in Wetland Mapping and Monitoring. In B. Huang (Ed.), *Comprehensive Geographic Information Systems* (Vol. 3, pp. 140-157). Elsevier Inc. https://doi.org/10.1016/B978-0-12-409548-9.10460-9

Zhang, L., Wu, B., Yin, K., Li, X., Kia, K., & Zhu, L. (2015). Impacts of Human Activities on the Evolution of Estuarine Wetland in the Yangtze Delta from 2000 to 2010. *Environmental Earth Sciences, 73,* 435-447. https://doi.org/10.1007/s12665-014-3565-2